Available online at www.sciencedirect.com
ScienceDirect
Diamond & Related Materials 16 (2007) 236–242
DIAMOND AND RELATED MATERIALS
www.elsevier.com/locate/diamond

Room temperature dc electrical conductivity studies of electron-beam irradiated carbon nanotubes

S. Gupta [a,*], R.J. Patel [a], N. Smith [a], R.E. Giedd [a], D. Hui [b]

[a] Department of Physics, Astronomy, and Materials Science, Missouri State University, 901 S. National Ave., Kemper Hall 103 M, Springfield, MO 65897, USA
[b] Department of Mechanical Engineering, University of New Orleans, New Orleans, LA 70148, USA

Received 12 February 2006; received in revised form 23 March 2006; accepted 22 May 2006
Available online 5 July 2006

Abstract

The influence of electron-beam (E-beam) irradiation on the electrical (electronic) properties of single- (SW) and multi-walled (MW) carbon nanotube grown by microwave chemical vapor deposition is investigated. These films were subjected to a constant energy of 50 keV (50 A/cm^2) from a scanning electron microscope gun for 2.5, 5.5, 8.0, and 15 h continuously — such conditions resemble increased temperature and/or pressure regime, enabling a degree of structural fluidity. To assess the structural modifications and electrical properties, the films were analyzed before and after irradiation. The experiments show that with increased exposure to ≥8–9 h, occasionally found individual bundles of single-wall nanotubes tend to collapse or pinch, graphitize/amorphize, and oxidize within the area of the electron-beam focus. Dramatic improvement in the *I–V* properties for single-walled (from semiconducting to quasi-metallic) and relatively small but systematic behavior for multi-walled with increasing exposure is discussed in terms of the critical role of controlled introduction of defects. The contact resistance decreases by orders of magnitude when exposed to electron beam and for all of the measurements the values ranged between 80 Ω and 10 kΩ at room temperature. These results also indicated that multi-walled nanotubes tend to reach a state of saturation degradation assessed by four-probe conductivity measurements. It is suggestive that there may be local gradual re-organization, *i.e.* $sp^{2+\delta}$, sp^3 C ⇔ sp^2 C. More importantly, they provided a contrasting comparison between metallic/semiconducting (*single*/*double-wall*) and invariably metallic (*multi-wall*) carbon nanotubes.

Keywords: Chemical vapor deposition; Carbon nanotubes; Electron-beam irradiation; Electrical properties; Space applications

1. Introduction

In the family of carbon materials, diamond is known for its reputation being radiation resistant besides a range of outstanding physical properties (electronic, optical, mechanical, and chemical). Hence it is preferable over the other existing semiconductors used in harsh environments [1]. Carbon nanotubes (CNTs) in the family of nanostructured carbon materials and serving as a model example of nanoscience and nanotechnology, have attracted considerable attention because of their unique unsurpassable physical (chemical, mechanical, electronic transport) properties [2–4]. They are found in a wide variety of geometries with unique electronic features and the possibility of being either metallic (multi- and single-walled) or semiconducting (single-walled), depending merely on the geometrical aspects of their structure [2], is one of their most remarkable properties. Therefore, they represent a novel class of carbon-based conducting nanowires suitable for the investigation of mesoscopic electronic transport phenomena. Moreover, by manipulating their structure we can modify their physical properties. Carrying out this locally, *i.e.* by changing the structure only along a short section of the tube or just on an individual or a few shells, we could create devices that are highly interesting for dedicated experiments based on the nanoscale electronics. Furthermore, the great strength anticipated for defect-free carbon nanotubes [5,6] motivates us for an exploration of structural failure modes of these nanoscale carbon fibers. However, damaging the tubes with energetic particles and/or photons – collectively described as irradiation effects – can induce a more dramatic structural modification. We focus here on irradiation with electrons because of its relevance to electron microscopy studies. Electron irradiation offers a powerful tool to manipulate structure locally and serves as a terrestrial simulant for ground-based radiation studies [7].

* Corresponding author. Tel.: +1 417 836 8565; fax: +1 417 836 6226.
E-mail address: SGupta@MissouriState.edu (S. Gupta).

0925-9635/$ - see front matter © 2006 Elsevier B.V. All rights reserved.
doi:10.1016/j.diamond.2006.05.009

In general, electron-beam damage proceeds *via* two pathways: a) direct knock-on collisions of electrons with atomic nuclei and b) radiolytic displacement mediated by beam-induced electronic excitations [7]. Up to the present time, several experiments have been conducted for the manipulation of nanotubes by energetic particles [8], but some open questions and challenges remain: i) nanoscale or even Ångstrom scale manipulation; ii) detailed structural characterization to understand the collapse or failure or modification of nanotubes; iii) forming novel carbon nanostructures [7], and moreover, it suggests that planar graphite may not be the most stable allotrope of carbon in systems of limited size thought earlier. Finally, one of the purposes of this research work is to develop advanced materials for space applications with characteristics such as light weight and compact, more absorption and/or dispersion, reduced single event effects besides other requirements such as strength, thermal, and hardness, offering multi-functionality [9]. For space and other applications such as safety of nuclear facilities, that they are physically stable and structurally unaltered when subjected to irradiation is indispensable.

The carbon nanotubes, which are the focus of the present studies, were subjected to relatively low energy [50 keV (or current density of 50 A/cm^2)] electron-beam irradiation continuously. Unlike the case of high energetic particles of hundreds of keV from the field emission transmission electron microscope used by several groups [10], the limitation of relatively low energy electron bombardment from traditional scanning electron microscope is overcome by several hours of irradiation exposures. Microstructural and electrical (electronic) property characterizations are made before and after irradiation to establish *property–structure* correlation. They include scanning electron microscopy (SEM) and current *versus* voltage (*I–V*) measuring resistivity (alternatively conductivity). The electronic density of states is also measured using ultra high vacuum scanning tunneling microscopy (UHV-STM). The damage or structural alteration in carbon nanotubes is found to be strongly dependent upon the number of irradiation exposure hours. Experimental studies showed that multi-walled nanotubes tend to be relatively more radiation resistant than those of single-walled nanotubes. This is because increased exposure on an occasionally found individual bundles of single-wall nanotubes tended to graphitize, pinch, and crosslink similar to polymers forming intra-molecular junction (IMJ) within the area of electron-beam focus, which is possibly through aggregates of amorphous carbon. It is also suggestive that there may be local gradual re-organization. Dramatic improvement in the *I–V* properties for single-walled nanotubes (from semiconducting to quasi-metallic) and relatively small but systematic behavior for multi-walled nanotubes with increasing irradiation is discussed in terms of the critical role of defects. More importantly, these findings provided a contrasting comparison between the single- and multi-walled nanotubes.

2. Experimental details

Films of carbon nanotubes for investigating the influence of electron-beam irradiation were prepared following the method described elsewhere [11,12]. Briefly, films of vertically aligned multi- and single-wall carbon nanotubes were synthesized using microwave plasma-enhanced chemical vapor deposition (MW CVD) employing acetylene and ammonia gas mixtures in 1:4 ratio at relatively higher deposition temperatures (*circa* 900 °C) using an iron (Fe) layer as catalyst on (SiO_2/Si) substrates deposited using electron-beam evaporation. Depending upon the Fe layer thickness (0.5 and 80 nm), the deposition resulted in the formation of single- and multi-wall nanotubes (SWNT and MWNT). The SiO_2 layer (~ 180 nm) was used as a diffusion barrier preventing reaction between Si and Fe forming silicides (*e.g.* $FeSi_2$, etc.). Deposition continued for <30–300 s for all of the samples. Pristine CNT samples were characterized using scanning electron microscopy (SEM (see Fig. 2a, c, and d). The samples were also characterized using Raman spectroscopy (RS) [although not shown for brevity and to avoid ambiguities] [13]. SEM images were obtained on JEOL 6400 with beam energy of 5 kV to investigate surface morphology. For irradiation experiments, these films were subjected to continuous electron beam from scanning electron microscope focused around 50–100 nm in diameter with beam current densities up to 10^4 A/cm^2, depending upon the diameter (scales as the inverse square of beam diameter). An electron energy of 50 keV, flux of ~ 10^{22} electrons/cm^2 was applied throughout the experiment in the sample area of 1×1 μm^2 (and 0.5×0.5 μm^2) and even smaller giving rise to an energy density of 50 A/cm^2 for 2.5, 5.5, 8.0, and 15 h continuously at ambient temperature. For current *versus* voltage (*I–V*) data, Keithley Model 236 and Model 6517 were used as the voltage source and ammeter, respectively. The Pt metal needle/tip of the atomic force microscope was used as an electrical contact probe with average area of 3 μm^2 spaced from each other by 150 μm. A typical schematic of the experimental set-

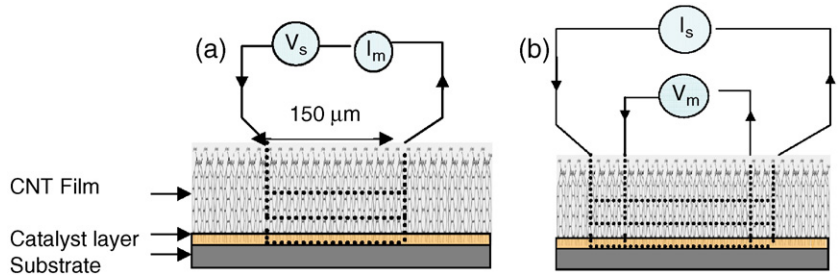

Fig. 1. (Color online). Schematic of (a) two- and (b) four-terminal set-up measuring electrical resistance. The electrodes serve as a voltage source (V_S), current probe (I_m), and current source (I_S).

up for two-terminal electrical properties measurements is shown in Fig. 1, which was extrapolated to traditional four-probe conductivity measurements.

For the scanning tunneling microscopy measurements, the samples were transferred into the UHV chamber pressure below 2×10^{-10} mbars. A commercial Omicron VT-STM (UHV-STM) was used. For spatial measurements, the mechanically prepared tungsten STM tip is biased to a certain voltage and is scanned over the sample surface, and its height is controlled by interrupting the feedback to give a constant tunneling current (I) mode, which allows the topographic imaging of the sample surface. STM images were collected from a sample area of 1×1 μm^2 with 100×100 raster points, and out of these 40×40 points were used for spectroscopy (STS). Given that the STS technique is quite sensitive to both the tip and sample surface structure, we were careful to present only those which are truly representative of the surface studied. In this respect, we have measured I–V curves on a few samples and at various positions on each sample. In STS, the tip is held at a fixed height above some position on the sample and the tunneling current (I) to the tip is measured as a function of the tip or sample bias (V). Since the tunneling current depends upon the electronic density of states (EDOS) of the tip and the sample, given the metallic nature of the tip (*i.e.* tungsten, the EDOS of the tip does not influence the overall shape of the specimens' EDOS. The magnitude of the tunneling current provides a measure of the local EDOS.

3. Results and discussion

Fig. 2 displays scanning electron micrographs revealing the morphology of the top surface of pristine and electron-beam irradiated multi- and single-walled carbon nanotubes. The multi-walled nanotubes show complicated morphology and appear to be random (see Fig. 2a), unlike single-walled nanotubes, which are smoother and appear to be 'carpet-like' (see Fig. 2c and d). The diameters estimated from high-resolution transmission electron microscopy for these tubes were ~ 1–4 nm for 0.5 nm Fe layer (SW) and ~ 100 nm (MW) for the 80 nm Fe layer and of several microns in length [12]. The films also contain some carbonaceous particles and it was found that the SW had much less impurity than those of MW nanotubes [12]. Just like multi-wall nanotubes, single-walled nanotubes tend to form bundles of nearly parallel tubules (appeared as a regular two-dimensional hexagonal lattice structure), although single isolated bundles can also be found *albeit* occasionally (see Fig. 2d). No apparent changes are observed in the SEM micrographs for the MW nanotubes even after continued exposure for 15 h (see Fig. 2a and b). In contrast, the SW nanotubes showed an apparent collapse or 'fusion' of a bundle, containing a few tubes in the irradiated area, which graphitizes, and most likely transforms into multi-walled with slight deposits or aggregation of amorphous carbon; a-C (see Fig. 2d and e) as addressed later in detail. It is also likely that the whole tube/bundle may not coalesce, but held together by a small aggregate of a-C in the irradiated area. In such a way, a coherent

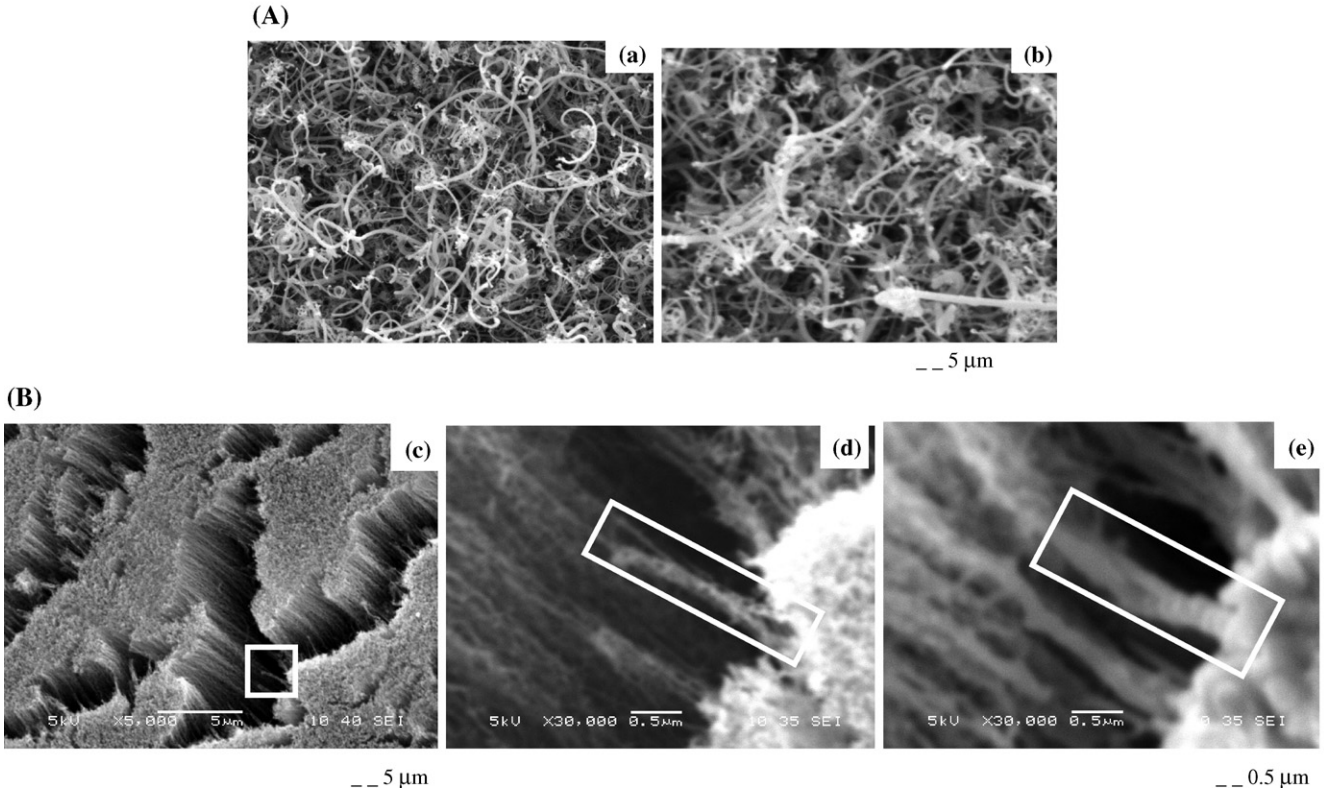

Fig. 2. Shown are the scanning electron micrographs of the top surface of (A) vertically aligned multi-wall and (B) single-wall carbon nanotube films (a, c, d) before and (b, e) after irradiation for 15 h continuously. Notice the collapse and aggregation of a-C layer of an isolated bundle of single-wall nanotube after 15 h of exposure (marked rectangular).

junction between SW and MW tubes can be formed which is useful for dedicated nano-electronic devices [7]. For electron energies employed hereby, the primary radiation effect in graphitic or sp^2 C materials is given by knock-on collisions of atoms with electrons, which leads to the generation of vacancies and interstitials (or structural defects). Since vacancies are almost immobile, they induce bending and curvature of graphene layers. Interstitials on the other hand, are much more mobile and invoke re-organization of the atoms' self-organization [13]. Qualitatively speaking, since multi-walled nanotubes did not reveal an apparent change in their surface morphology even after 15 h of exposure in contrast to single-walled nanotubes, it implies that the former tend to be relatively more robust or alternatively 'radiation resistant' [14]. For further analyses and to establish a property–structure correlation, we characterized their electrical (electronic) properties: contact resistance (or two-terminal resistance; R_{2t}) and internal resistance (four-probe; R_{4t}). MW nanotubes have certain specific advantages over SW: their large diameter favors low ohmic contacts, ascribed to larger contact area.

One can view carbon nanotubes as giant conjugated molecular wires with a conjugation length corresponding to almost the whole length of the tube. Whether a pristine nanotube conducts electrons as a quantum wire or behaves as an exceptional semiconductor is determined by its diameter and chiral angle, uniquely indexed with two integers (n, m). [For MWNTs one expects a more complicated situation, because of a possible additional electronic coupling between adjacent shells]. This prediction is usually verified by mesoscopic electrical transport measurements [15]. On a more fundamental level, the electronic properties of these one-dimensional (1D) conductors have generated much interest. The reason for this excitement lies in their rich phase diagram and the prediction that in a 1D system the Coulomb interaction should lead to a strongly correlated electron gas, called a Luttinger liquid instead of the weakly interacting quasi-particles described as a Fermi-liquid in conventional metals. This issue is still controversial and understanding is at a rudimentary level [16]. E-beam irradiation induces defects and (perhaps) structural deformations affecting their electronic behaviors.

Herein, we demonstrate that two-and four-terminal resistance determining contact and internal resistance, respectively is quite sensitive to electron-beam irradiation. A series of room temperature current *versus* voltage (I–V) measurements for both the MW and SW as a function of E-beam exposure time are displayed in Fig. 3. All of these measurements determine two-terminal resistance: R_{2t} summarized in Fig. 4. It is worthy to note that the abscissa also translates into the level of dose. In general, the factors which affect the variation in resistances of CNTs are: (a) the quality of the nanotubes; (b) the fabrication technique applied to electrically address the nanotube; and (c) the quality of the electrical contacts. Research on semiconductor devices has shown that the formation of Schottky barriers may render the realization of low-ohmic contacts rather difficult. Here, we used a metal tip as the electrical contact probe. Quantitatively, the R_{2t} decreases substantially by almost three orders of magnitude for the most irradiated from an initial value for both (MW and SW) (*i.e.* from 80 to 10 kΩ) nanotubes. This experimental finding implies that E-beam exposure reduces the electrical contact resistance of nanotubes substantially which is similar to the results reported earlier [17]. It offers an opportunity rather than a limitation. It is this localized degradation that improves contact behavior, which plays a crucial role in future research and application of carbon nanotubes in nanoelectronic devices. They are useful both as active device elements (Schottky diodes) and as an electrical contact to semiconductor devices (metal-semiconductor). It seems MW becomes more metallic with extremely low contact resistance with high defect density. [The current for the MWNT was too high to be measured]. The rapid decrease of contact resistance is a direct consequence of defect creation/accumulation. The R_{2t} starts to saturate for MW, unlike for SW as shown in Fig. 4a. The fact that R_{2t} in Fig. 4a does not (yet) saturate for the largest irradiation hours indicates that a further decrease is perhaps possible, which can be facilitated by possibly selecting a smaller window containing only a few SW tubes. In our case, however, the intensity saturation at the highest irradiation must reflect changes in defect dynamics. It seems that there may be a critical concentration of defects beyond which the defect production is not favorable and the additional defects are cured.

Although the exact mechanism for the remarkable decrease of R_{2t} is unclear, but we propose the following plausible origins: first, a contamination of a-C deposited during the exposure may

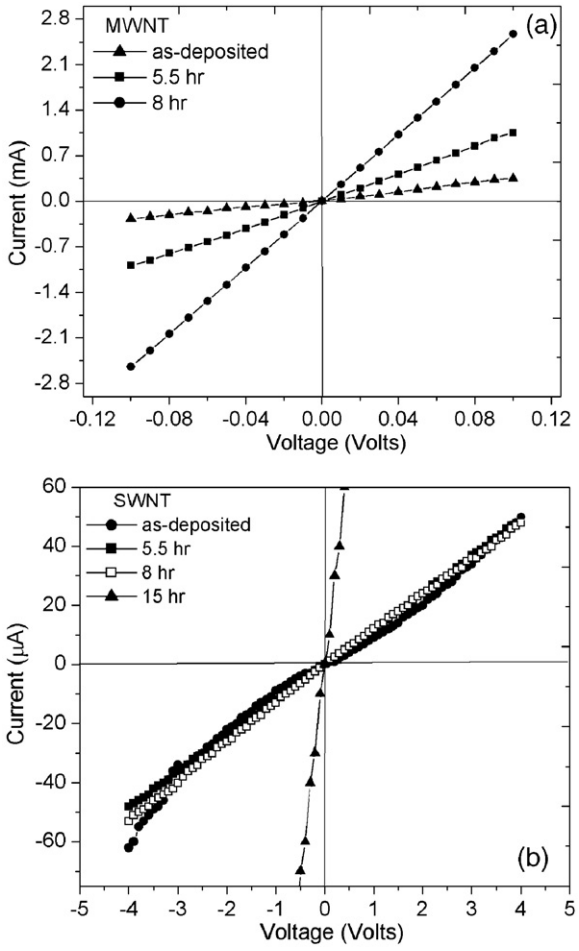

Fig. 3. Shown is the room temperature current *versus* voltage (I–V) plots for (a) multi-walled and (b) single-walled carbon nanotubes as a function of electron-beam irradiation exposure time.

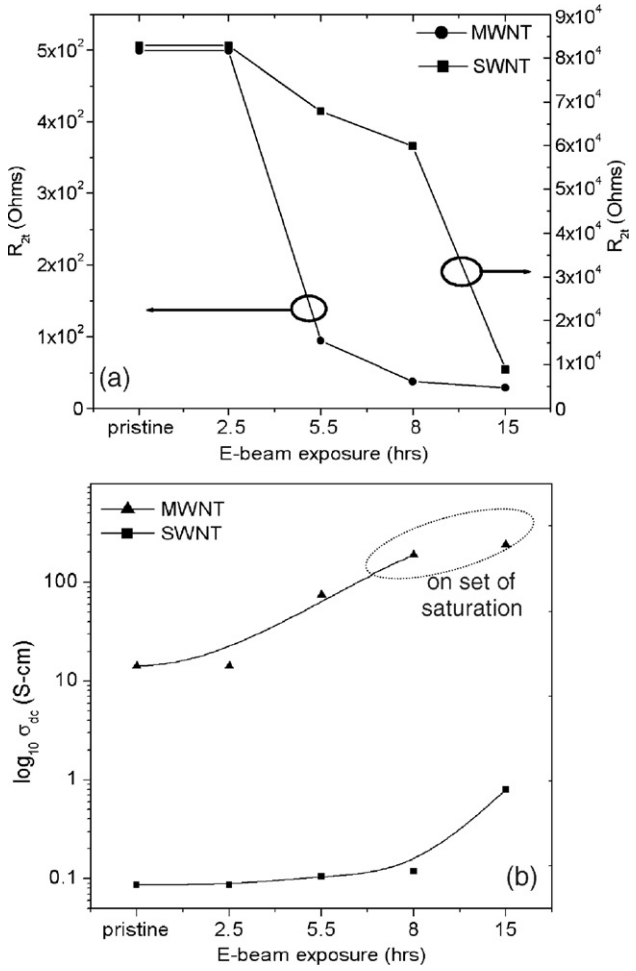

Fig. 4. (a) Variation of two-terminal (R_{2t}) resistance for multi- and single-walled carbon nanotubes with electron-beam irradiation hours (b) corresponding dc conductivities obtained using four-probe measurement.

reduce the measured contact resistance. Second, the electrical contacts between the nanotube and Pt needle may have been improved considerably rather locally. Finally, E-beam may have induced local nanotube modification which has introduced structural/chemical defects resulting in low contact resistance. The fact that SW nanotube contact resistance decreases, implies that the nanotube itself is not destroyed, or else the reverse would have occurred.

To demonstrate that the nanotube itself is left relatively unaltered if exposed with low energy electron beam for many hours continuously or unexposed, the intrinsic resistance is measured using four-terminal on a nanotube bundle. We used AFM equivalent Pt tip to locally probe the electrical properties of CNTs. [Pt usually probes the high-resistance contact with slight Schottky barrier]. Using the tip as a voltage probe and the other set as the current source, we study the properties of the contacts and they can be extrapolated to internal resistance of the tubes determining R_{4t}, which was used to determine dc electrical conductivity (inverse of four-probe resistivity) [see Figs. 1 and 4b]. There are strong correlations between the microstructural changes that can be deduced from the electrical conductivity and the number of irradiation hours. Pristine SW films were primarily semiconducting in nature reflected in its I–V behavior which appears to be diode-like with much less defect density. Moreover, these observations point out that the MW becomes more and more metallic and SW is transiting from semiconducting to quasi-metallic in electronic character (see Fig. 4b). The intrinsic resistance for pristine MW and SW nanotubes was of the order of a few k-ohms, which starts to diminish rather weakly with increasing irradiation. This is perhaps a direct consequence of defect aggregation apparent from SEM micrographs for SW nanotubes, in particular. The reason that the electrical conductivity of a nanotube bundle increases at higher radiation dose is attributed to the localization of conducting electrons by defects and/or forming covalent bonds between adjacent nanotubes. These findings partially comply with those reported earlier [18,19], although systematic studies with temperature are left open for future work [18]. Our investigations have shown that investigating the electrical transport in MW is somewhat similar to the larger diameter SW. The current mainly flows on the external cylinder and the nanotube core solely acts as a mechanical support for the electrically active outermost shell. (Notice that this may no longer be true if we could find a way to contact the core or to selectively address inner shells).

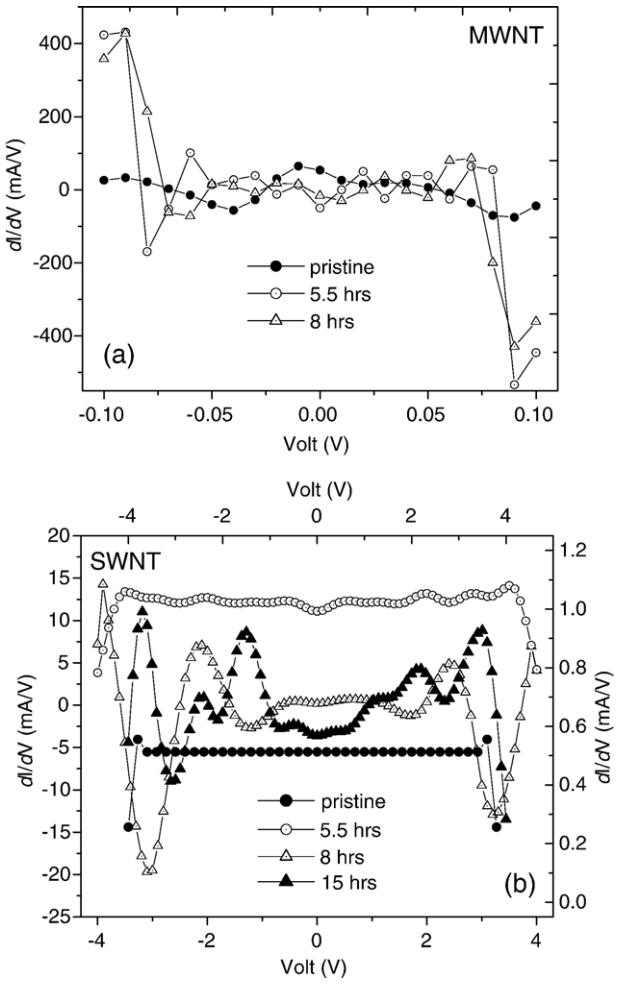

Fig. 5. Differential conductance (dI/dV) *versus* sample voltage (V) calculated from the data shown in Fig. 3.

Fig. 5 shows the two-terminal differential conductance (dI/dV) *versus* voltage (V) of the corresponding Fig. 3. These plots show apparently some similarity with the results obtained using scanning tunneling spectroscopy (STS), which offers another means to probe electronic structure with nanometer spatial resolution [14,20,21]. For spatial measurements, the STM tip is biased to a certain voltage and scanned over the sample surface. Its height is controlled by the feedback in order to give a constant tunnel current which allows topographic imaging of the sample surface. In STS, the tip is held at a fixed height and the tunnel current (I) to the tip is measured as a function of the tip or sample voltage (V). The tunneling current depends upon the electronic density of states (EDOS) of the tip and the sample. However, given the metallic nature of the tip the EDOS of the tip does not influence the overall shape of the specimens' EDOS. A typical example of I–V (tunneling current *versus* sample voltage) and differential conductance; dI/dV is provided in Fig. 6 for pristine SW and MW nanotubes. I–V characteristics exhibit a plateau at zero current for tubes with an average diameter of ~ 1.28 nm. This rectifying behavior is the signature of semiconducting nature of the tubules unlike MW, which are invariably metallic with finite resistance. The dI/dV shown in Fig. 5b *crudely* mimics 1D electronic density of states in ambience and it is analogous to those shown in Fig. 6c. The peaks in dI/dV being attributed to $1/(E_0-E)^{1/2}$ type singularities in the 1D EDOS. Several I–V curves were collected and the spectra were quite reproducible. The scatter in the data (Fig. 5) accounts for the surface contamination, structural and chemical defects. The large bias voltage dependence of dI/dV, however is notably different. These observations are undoubtedly compelling and discussed in terms of the role of defects. Defects generated by electron irradiation modify the electronic structure near the Fermi level (see Fig. 6c) and affect the electrical resistivity of carbon nanotubes as discussed above. On careful examination, the peaks for both the samples exposed to 8 and 15 h show prominent peaks in addition to the narrowing or closing band gap due to defects presumably for the latter. We note that Fig. 6c is also a measure of the energy band gap (indicated by arrow), according to which the SW (mixed metallic and semiconducting) have larger band gap than those of MW (invariably metallic) nanotubes. Nonetheless, the defects created by E-beam destroy the coherent motion of atoms (lowering the spatial coherence of electron waves) on the nanotube and increase or saturate their resistivity [22].

As suggested in Ref. [17], we have identified the structural/electrical transformation in carbon nanotubes from multi- to multi-walled (metallic→metallic) and single- to quasi-multi-walled (semiconducting→more metallic) with disorder. An important new aspect of irradiation in nanostructured carbons is realized, where the solid is far from thermal equilibrium (non-equilibrium) and under certain circumstances it can fulfill the conditions of self-organized structure formation. Accordingly, the change of hybridization facilitates the structural transformation, *i.e.* $sp^{2+\delta}$, $sp^3 \Leftrightarrow sp^2$, $sp^{2+\delta}$ (Trigonal ⇔ mixed Trigonal, Tetrahedral). Moreover, the difference in the behaviors of SW to those of MW may be due to structural differences (MW is closer to graphite).

The prospects for nanotube-based electronics are fascinating and huge, but far from practicality — several issues need to be resolved. Overall, the nanotube presents all the desirable properties needed for future electronic applications. Furthermore, to investigate the usefulness of the present technique for making contacts in a nanotube network measuring the electrical properties of such a coherent junction between SW and MW would be a challenge for future investigations. Despite these efforts,

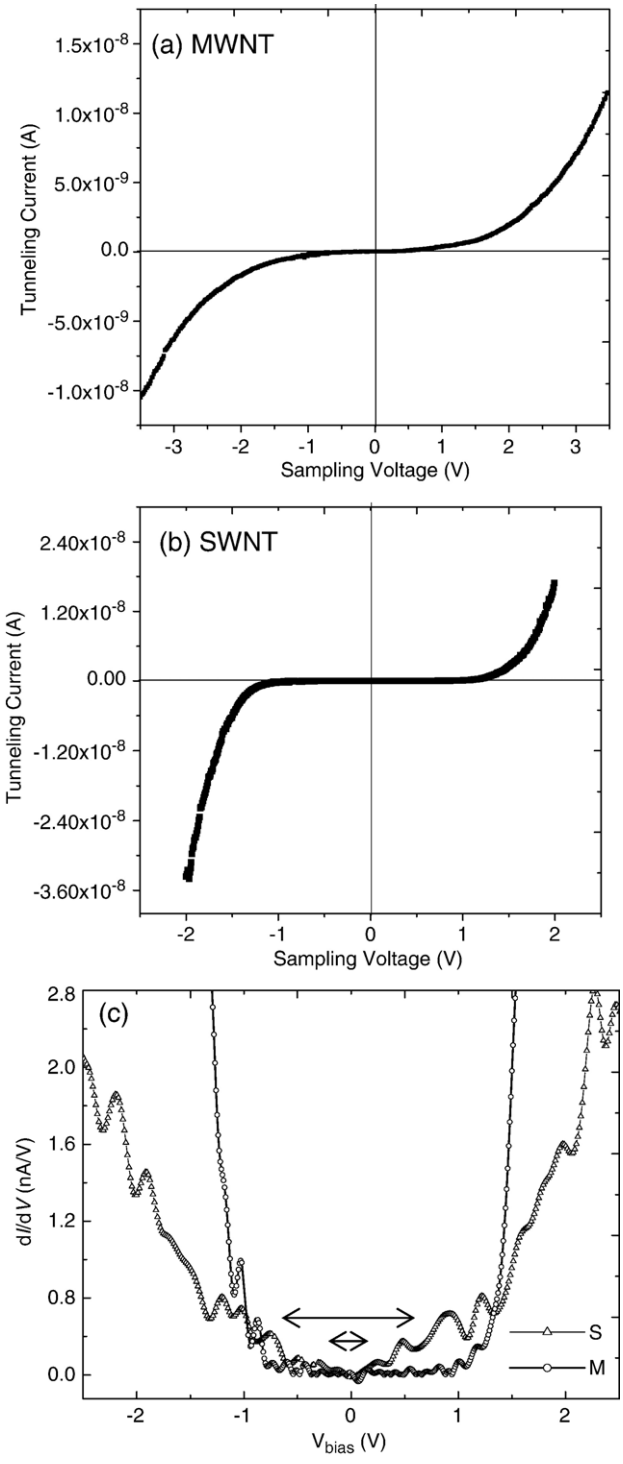

Fig. 6. Tunneling current (I) *versus* sample voltage (V) measured using UHV-STM of the pristine (a) MW and (b) SW carbon nanotubes demonstrating (quasi) metallic and semiconducting nature, respectively. (c) Differential conductance (dI/dV) *versus* sample voltage (V) applied showing an apparent similarity with Fig. 5.

underpinning the precise nature of electrical (electronic) properties of electron-beam modified nanotubes is beyond the scope of the present measurements, but probably will be a key to understanding the mechanisms involved. As a general remark, the electrical transport properties across interfaces remain poorly understood in terms of science/predictive capability, affecting all of the nanomaterials and motivates us to pursue such investigations in detail in the future.

4. Conclusions

In summary, we investigated the influence of electron-beam irradiation on the multi- and single-walled nanotubes surface assessed through room temperature electrical properties measurements in addition to in situ imaging. We showed how nanotubes can be tailored with high precision under a focused electron beam. According to our present understanding, it appears that MW tends to be relatively more structurally stable (alternatively, radiation resistant) than that of SW which tends to collapse, graphitize, and deposit aggregates of a-C for extended exposure. Dramatic improvement in the *I–V* properties for single-walled (from semiconducting to quasi-metallic) and relatively small but systematic behavior for multi-walled nanotubes (from metallic to more metallic) with increasing irradiation exposure hours is discussed in terms of the critical role of defects aggregation. These results indicated that multi-walled nanotubes tend to reach a state of defect density saturation unlike single-walled nanotubes. It was also suggestive that knock-on collision may not be the primary cause of structural degradation, rather a local gradual reorganization, *i.e.* $sp^{2+\delta}$, sp^3 C $\Leftrightarrow$ sp^2 C. These studies allowed favorable electrical contacts through local 'soldering'. These results are unprecedented and demonstrate a contrasting comparison between single- and multi-walled nanotubes. Furthermore, to investigate the usefulness of the present technique for making contacts in a nanotube network, measuring the electrical properties of such a coherent junction between SW and MW would be a challenge for future studies.

Acknowledgements

The corresponding author (SG) is thankful for having used the facilities (SEM) housed in the Center for Applied Science and Engineering at the Missouri State University, to Drs. R. J. Nemanich and Y. Y. Wang for sharing some of the nanotube films, Mr. J. Tedesco (for STM measurements) [NC State University, Raleigh] and for the financial support through internal funds.

References

[1] S. Gupta, B.L. Weiss, B.R. Weiner, L. Pilione, A. Badzian, G. Morell, J. Appl. Phys. 92 (2002) 3311 (and references therein).
[2] M.S. Dresselhaus, G. Dresselhaus, P.C. Eklund, Science of Fullerenes and Carbon Nanotubes, Academic Press, New York, 1996. R. Saito, G. Dresselhaus, M.S. Dresselhaus, Physical Properties of Carbon Nanotubes, Imperial College Press, London, 1998;
M.S. Dresselhaus, G. Dresselhaus, R. Saito, Phys. Rev., B 45 (1992) 6234.
[3] C. Dekker, Phys. Today 52 (1999) 22.
[4] R.H. Baughman, A.A. Zakhidov, W.A. de Heer, Science 297 (2002) 787.
[5] V.H. Crespi, N.G. Chopra, M.L. Cohen, A. Zettl, S.G. Louie, Phys. Rev., B 54 (1996) 5927.
[6] N.G. Chopra, L.X. Benedict, V.H. Crespi, M.L. Cohen, S.G. Louie, A. Zettl, Nature 377 (1995) 135.L.X. Benedict, V.H. Crespi, N.G. Chopra, M.L. Cohen, S.G. Louie, A. Zettl (unpublished).
[7] F. Banhart, Rep. Prog. Phys. 62 (1999) 1181.
[8] J. Li, F. Banhart, Nano Lett. 4 (2004) 1143.
[9] J.W. Wilson, F.A. Cucinotta, M.-H.Y. Kim, W. Schimmerling, Phys. Med. XVII (Sept. 2001) 67.
[10] D. Ugarte, Nature 359 (1992) 707. D. Ugarte, Chem. Phys. Lett. 207 (1993) 473.
[11] Y.Y. Wang, G.Y. Tang, F.A.M. Koeck, Billyde Brown, J.M. Garguilo, R.J. Nemanich, Diamond and Relat. Mater. 13 (2004) 1287.
[12] Y.Y. Wang, S. Gupta, R.J. Nemanich, Appl. Phys. Lett. 95 (2004) 2601.
[13] S. Gupta, R.J. Patel, N. Smith, R.E. Giedd, J. Mater. Res. (in press).
[14] J.W.G. Wildoer, L.C. Venema, A.G. Rinzler, R.E. Smalley, C. Dekker, Nature (Lond.) 391 (1998) 59.
[15] M. Bockrath, D.H. Cobden, P.L. McEuen, N.G. Chopra, A. Zettl, A. Thess, R.E. Smalley, Science 275 (1997) 1922 (and references therein).
[16] T.E. Odom, J.-L. Huang, J.-L. Kim, C.M. Lieber, Nature (Lond.) 391 (1998) 62 (and references therein).
[17] A. Batchold, M. Henny, C. Terrier, C. Strunk, C. Schönenberger, J.-P. Slavetat, J.-M. Bonard, L. Forró, Appl. Phys. Lett. 73 (1998) 274.
[18] László Forró, Christian Schönenberger, Europhys. News 32 (3) (2001).
[19] T.W. Ebbesen, H.J. Lezec, H. Hiura, J.W. Bennett, H.F. Ghaemi, T. Thio, Nature (Lond.) 382 (1996) 54.
[20] J. Risten, J. Schafer, L. Ley, Diamond and Relat. Mater. 4 (1995) 508.
[21] G. Binning, H. Rohrer, C. Gerber, E. Weibel, Appl. Phys. Lett. 40 (1981) 178.
[22] M. Hulman, V. Skákalová, S. Roth, H. Kuzmany, J. Appl. Phys. 98 (2005) 24311 (and references therein).